

Article

Quantum Chemical Studies and Electrochemical Investigations of Polymerized Brilliant Blue-Modified Carbon Paste Electrode for In Vitro Sensing of Pharmaceutical Samples

Pattan-Siddappa Ganesh ¹, Sang-Youn Kim ^{1,*} , Savas Kaya ^{2,*}, Rajae Salim ³, Ganesh Shimoga ¹ and Seok-Han Lee ¹

¹ Interaction Laboratory, Future Convergence Engineering, Advanced Technology Research Center, Korea University of Technology and Education, Cheonan-si 31253, Chungcheongnam-do, Korea; ganeshps11@koreatech.ac.kr (P.-S.G.); shimoga@koreatech.ac.kr (G.S.); shlee@koreatech.ac.kr (S.-H.L.)

² Department of Pharmacy, Health Services Vocational School, Sivas Cumhuriyet University, Sivas 58140, Turkey

³ Laboratory of Engineering, Organometallic, Molecular and Environment (LIMOME), Faculty of Science, University Sidi Mohamed Ben Abdellah, P.O. Box 1796, Fez 30000, Morocco; salimrajae@gmail.com

* Correspondence: sykim@koreatech.ac.kr (S.-Y.K.); savaskaya@cumhuriyet.edu.tr (S.K.); Tel.: +82-(0)41-560-1484 (S.-Y.K.)



Citation: Ganesh, P.-S.; Kim, S.-Y.; Kaya, S.; Salim, R.; Shimoga, G.; Lee, S.-H. Quantum Chemical Studies and Electrochemical Investigations of Polymerized Brilliant Blue-Modified Carbon Paste Electrode for In Vitro Sensing of Pharmaceutical Samples. *Chemosensors* **2021**, *9*, 135. <https://doi.org/10.3390/chemosensors9060135>

Academic Editor: Edward P. C. Lai

Received: 30 April 2021

Accepted: 8 June 2021

Published: 10 June 2021

Publisher's Note: MDPI stays neutral with regard to jurisdictional claims in published maps and institutional affiliations.



Copyright: © 2021 by the authors. Licensee MDPI, Basel, Switzerland. This article is an open access article distributed under the terms and conditions of the Creative Commons Attribution (CC BY) license (<https://creativecommons.org/licenses/by/4.0/>).

Abstract: To develop an electrochemical sensor for electroactive molecules, the choice and prediction of redox reactive sites of the modifier play a critical role in establishing the sensing mediating mechanism. Therefore, to understand the mediating mechanism of the modifier, we used advanced density functional theory (DFT)-based quantum chemical modeling. A carbon paste electrode (CPE) was modified with electropolymerization of brilliant blue, later employed for the detection of paracetamol (PA) and folic acid (FA). PA is an analgesic, anti-inflammatory and antipyretic prescription commonly used in medical fields, and overdose or prolonged use may harm the liver and kidney. The deficiency of FA associated with neural tube defects (NTDs) and therefore the quantification of FA are very essential to prevent the problems associated with congenital deformities of the spinal column, skull and brain of the fetus in pregnant women. Hence, an electrochemical sensor based on a polymerized brilliant blue-modified carbon paste working electrode (BRB/CPE) was fabricated for the quantification of PA and FA in physiological pH. The real analytical applicability of the proposed sensor was judged by employing it in analysis of a pharmaceutical sample, and good recovery results were obtained. The potential excipients do not have a significant contribution to the electro-oxidation of PA at BRB/CPE, which makes it a promising electrochemical sensing platform. The real analytical applicability of the proposed method is valid for pharmaceutical analysis in the presence of possible excipients. The prediction of redox reactive sites of the modifier by advanced quantum chemical modeling-based DFT may lay a new foundation for researchers to establish the modifier–analyte interaction mechanisms.

Keywords: carbon paste electrode; Fukui functions; electrostatic potential map; electrochemical sensing; pharmaceutical samples; excipients; folic acid; paracetamol

1. Introduction

Electroanalytical methods are promising in the estimation and determination of neurotransmitter amines, inorganic and organic molecules and pharmaceutical samples in biotic and/or pharmacological fluids [1–3]. Among the other analytical techniques, electroanalytical approaches have principal advantages such as sensitivity, high resolution, a quick operating procedure and selectivity towards the quantification of the target analyte [4,5]. In order to benefit from all the advantages of electroanalytical methods, the choice of working electrode plays a very significant role in developing a sensor. Among the carbon-based

working electrodes, the carbon paste working electrode (CPE) is an appropriate conductive matrix, having features such as a wide-ranging potential window, quick preparation through mechanical mixing with suitable surface reformation and less background current during analysis [6–8]. However, bare working electrodes are associated with unavoidable drawbacks such as a slow electron transport rate, poor resolution in binary/ternary mixture analysis and major fouling of the electrode surface [9,10]. However, electrochemistry scientists have demonstrated many acceptable methodologies to improve the performance of the bare electrode through modification of the working electrode [11–13]. There are so many different materials used in the literature to modify the working electrode, such as nanoparticles/composites [14], multiwall carbon nanotubes [15], organic compounds [16], ionic liquids [17] and surfactants [18].

Paracetamol (acetaminophen, PA) is an analgesic, antipyretic and anti-inflammatory medicine used for the treatment of mild to moderate fever caused by viral and/or bacterial infections. In addition, it is also used to get relief from pain related to headache, arthritis and post-operative pain [19,20]. Usually, oral administration of PA will not cause any side effects in low doses. However, overdose may lead to infection of the pancreas, glutathione depletion, kidney destruction, hepatotoxicity and gastritis [21]. Oral intake of PA in children may cause an increased chance of asthma, eczema and rhino conjunctivitis [22]. Therefore, the development of a sensor for PA is of great importance and has attracted attention among researchers. Folic acid (folate, FA) is a water-soluble part of vitamin B complex, has a crucial role in biological systems and is essential for the growth and differentiation of cells [23]. The natural resources of folate are vegetables, fresh fruit, yolk and liver. To prevent megaloblastic anemia in pregnant women, daily supplementation of folic acid is highly recommended [24]. Deficiency in folic acid may cause neural tube defects, mental devolution, congenital anomalies of the spine and brain and fetal development defects [25]. As a result, determining PA and FA independently or simultaneously plays an important role in early clinical diagnosis. Moreover, both PA and FA are electrochemically active; therefore, electroanalytical detection is the best possible method due to its cost-effectiveness, ease of preparation, sensitivity and selectivity. Conventional bare working electrodes show a poor response due to slow electrode kinetics. Hence, chemically modified working electrodes were established in recent years to overcome this problem [26,27]. Brilliant blue (BRB) is a simple organic triarylmethane dye used for staining purposes in biochemical analysis and also as a colorant in the food industry. Recently, in 2018, Devi et al. reported a new methodology for direct electrochemical sensing of triazophos pesticide by fabricating a brilliant blue dye surface-confined carbon black nanoparticle-modified electrode [28]. Chen et al. prepared a brilliant blue FCF-modified working electrode to study the electrocatalytic behavior of L-Cysteine and oxygen [29]. A report on the protocol to modify CPE by brilliant blue for the simultaneous interference-free determination of dihydroxy benzene isomers was presented in [30]. From these reports, it can be seen that there is a curiosity among electroanalytical researchers to develop a brilliant blue-based electrode for sensing applications [28–30]. There are too many research papers on the electropolymerization technique's modification of the working electrode with the assumption that a thin layer of the modifier coating is formed on the surface of a working electrode, which then serves as an electron transfer mediator by increasing the working electrode surface area. However, locating the active redox reactive sites on the modified electrode is critical for a better understanding of the sensing process, which has remained unclear in all previous studies involving modified carbon paste electrodes made by electropolymerization [7,16,24,30]. Recently, very few reports to predict the mediating mechanism of the modifier have been proposed [31–33]. In the continuation of our research, the present work demonstrates the fabrication of a cost-effective and analytically applicable electrochemical sensor for the detection of PA and FA individually as well as simultaneously. The brilliant blue was electropolymerized on the conductive carbon paste working electrode, followed by electrochemical and surface texture characterization. We adopted an advanced density functional theory (DFT) calculation to predict the redox

reactive sites of the modifier. Moreover, there were no reports on electroanalysis of PA and FA on the polymerized brilliant blue-modified carbon paste working electrode (BRB/CPE) by the CV technique. Overall, the fabricated BRB/CPE electrode showed an enhanced response for the electroanalysis of our targeted analytes. The prediction of redox reactive sites of the modifier by advanced quantum chemical modeling-based DFT may lay a new foundation for researchers to establish the modifier–analyte interaction mechanisms.

2. Experimentation

2.1. Reagents, Chemicals and Instrumentation

Paracetamol (PA) and coomassie brilliant blue R-250 (BRB) were purchased from Himedia, and stock solutions of 2.5 mM and 25.0 mM were prepared in double-distilled water. Folic acid (FA) was procured from Himedia, and 2.5 mM solution was prepared in 0.1 M NaOH solution. Sodium phosphate buffer solution (SPBS) of the favored pH was obtained by appropriate mixing of 0.2 M $\text{NaH}_2\text{PO}_4 \cdot \text{H}_2\text{O}$ and 0.2 M Na_2HPO_4 solutions. All the reagents, chemicals and solvents were of analytical grade and used as received. The scanning electron microscopy (SEM) images were obtained using a ZEISS Ultra-55. All electrochemical experiments were performed with electrochemical workstation model CHI-660D. The three-electrode system used comprised a saturated calomel electrode (SCE) (reference), platinum wire (counter) and BCPE or BRB/CPE (working) electrode. All experiments were performed at a temperature of 25 ± 0.1 °C.

2.2. Preparation of Carbon Paste Electrode

In order to prepare the carbon paste electrode, we followed the previously reported literature [16,34]. The finely grinded 70% graphite powder and 30% silicone oil were hand mixed in a mortar until a homogenous thick paste was obtained. This paste was then transferred and tightly packed into the cavity of the carbon paste electrode (CPE) and then smoothed on a piece of paper, later named as bare carbon paste electrode (BCPE). A fresh electrode surface could be obtained by removing a small portion of the paste and polishing on the piece of paper until a smooth surface was observed.

2.3. Tablet Sample Preparation

Individual tablets containing PA (Dolo 500 mg, Micro Labs Limited, South Sikkim, India) and FA (Orofer XT, Emcure Pharmaceuticals Limited, Jammu, India) were bought from a pharmacy and directly analyzed by the CV technique after sample preparation. The manufacturer claimed 500 mg of PA and 1.5 mg FA content in their respective tablet formulations. Later, the tablets were weighed and finely crushed using a mortar and pestle, and an adequate quantity of this sample was dissolved with double-distilled water and sonicated for 30 min to ensure complete dissolution. Later, the solution was filtered to remove undissolved solids; the obtained supernatant solution was diluted with SPBS. The standard addition method was used for recovery studies.

2.4. Computational Methods

Quantum chemical calculation is an important method that can offer a large amount of information about structural properties and therefore predict their reactivity [35]. Thus, a DFT method based on the B3LYP/6-31G (d,p) base was executed using the Gaussian 09 program in order to estimate the reactivity of the brilliant blue molecule. The DFT concept introduced by Parr and Pearson led us to extract several descriptors of chemical reactivity such as chemical electronegativity (χ), hardness (η) and softness (σ) [36], in order to predict these quantum chemical descriptors. Pearson and Parr [37] suggested Equations (1)–(3), where $I = -E_{\text{HOMO}}$ is the ionization energy, and $A = -E_{\text{LUMO}}$ represents the electron affinity.

$$\chi = \left[\frac{\partial E}{\partial N} \right]_{v(r)} = - \left(\frac{I + A}{2} \right) \quad (1)$$

$$\eta = \frac{1}{2} \left[\frac{\partial^2 E}{\partial N^2} \right]_{v(r)} = \frac{I - A}{2} \quad (2)$$

$$\sigma = 1/\eta \quad (3)$$

The solvent effect investigation was included using the conductor-like polarizable continuum model (CPCM).

According to Gazquez and collaborators [38], the electro-accepting power (ω^+) and electro-donating power (ω^-) parameters which are conditional in ionization energy and electron affinity concepts can predict the electron-donating and electron-accepting abilities of studied chemical species (Equations (4) and (5)):

$$\omega^+ = (I + 3A)^2 / (16(I - A)) \quad (4)$$

$$\omega^- = (3I + A)^2 / (16(I - A)) \quad (5)$$

Generally, Fukui indices indicate the tendency of a molecule to give or obtain electrons. Therefore, these functions were modeled to detect the most nucleophilic interactions in a molecule [39]. The electrophilic (f_k^-) and nucleophilic (f_k^+) attacks were calculated using Equations (6) and (7), where P_k is the natural population for atom k site in the cationic ($N - 1$), anionic ($N + 1$) or neutral molecule (N):

$$f_k^+ = P_k(N + 1) - P_k(N) \quad \text{Nucleophilic attack} \quad (6)$$

$$f_k^- = P_k(N) - P_k(N - 1) \quad \text{Electrophilic attack} \quad (7)$$

3. Results

3.1. Fabrication of BRB/CPE and Its Electrochemical Characterization

The optimized protocol followed to fabricate a BRB/CPE is explained here. The 0.5 mM solution of brilliant blue in 0.1 M NaOH (supporting electrolyte) was taken in an electrochemical cell and was linearly swept between the potentials of -0.5 and 1.5 V for 15 consecutive cycles with a scan rate of 0.1 Vs^{-1} by the cyclic voltammetry (CV) technique. From Figure S1 (see Supplementary File), it can be observed that the increase in redox peak currents with increasing sweep cycles was the preliminary observation in the growth of the polymeric chain on the carbon past electrode. Later, the current response in the voltammogram after a few cycles becomes almost steady and later turns out to be constant. This reflects the saturation level in the electropolymerization phenomenon [30–32,40].

The critical performance and electrocatalytic ability of the BRB/CPE directly depend on the thickness of the polymeric film formed, and this can be meticulously controlled by varying the parameters while recording the voltammograms. Figure 1A shows the CVs for the electro-oxidation of $20.0 \mu\text{M}$ PA in SPBS (0.2 M, pH 7.4) at the BRB/CPE fabricated by different numbers of sweep cycles. From Figure 1B, it is clearly seen that the extreme current signal was obtained at 15 cycles of the modified electrode. Therefore, 15 cycles were chosen as a representative modification protocol to fabricate the BRB/CPE. The electroactive surface area of the working electrode was calculated by using the Randles–Sevcik equation, by recording the CV of $1.0 \text{ mM Fe}^{2+/3+}$ in 1.0 M KCl (supporting electrolyte) as a standard redox probe [16,40].

$$I_p = 2.69 \times 10^5 n^{3/2} A D^{1/2} C_0 v^{1/2} \quad (8)$$

where n is the number of electrons exchanged in the redox process (here $n = 1$). I_p (A), A (cm^2), D (cm^2/s), C_0 (mol/cm^3) and v (V/s) are the peak current, electroactive surface area, diffusion coefficient, concentration of electroactive species and scan rate, respectively. It was calculated that the BRB/CPE (0.0351 cm^2) has a more electroactive active surface area as compared to the BCPE (0.0289 cm^2).

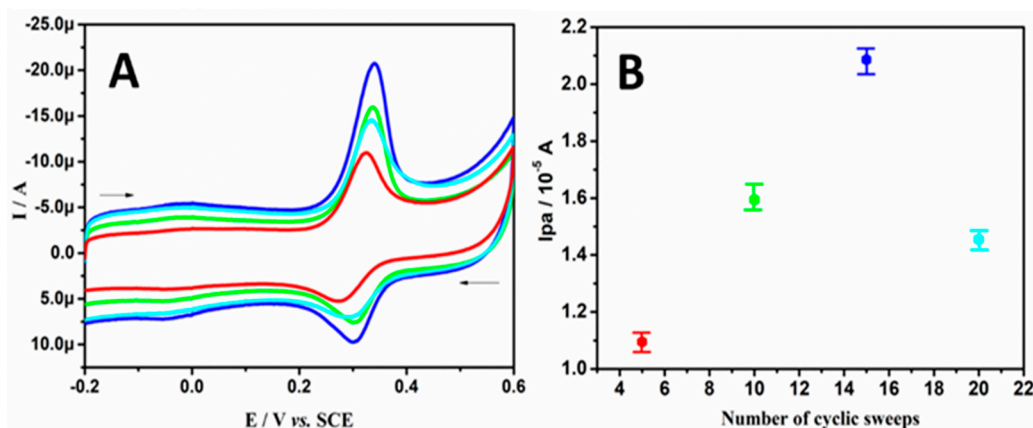


Figure 1. (A) CVs recorded for the electro-oxidation of 20.0 μM PA at BRB/CPE fabricated by different numbers of cycles. (B) Inset shows the graph of anodic peak current versus number of cyclic sweeps.

The amount of polymeric film adhered to the working electrode surface was calculated by Equation (9) [40,41].

$$I_p = n^2 F^2 A \Gamma v / 4RT \quad (9)$$

Here, Γ (mol/cm^2) is the surface coverage, and I_p (A), v (V/s) and A (cm^2) are the peak current, scan rate and area of the working electrode, respectively. F (C mol^{-1}), R ($\text{J K}^{-1} \text{mol}^{-1}$) and T (K) are significant universal constants, and n is the number of electrons exchanged. By substituting these values in Equation (9), Γ was calculated to be $0.31 \times 10^{-10} \text{ mol}/\text{cm}^2$. To understand the surface texture, the scanning electron microscopy (SEM) images of the BCPE (a) and BRB/CPE (b) are shown in Figure 2. The BRB/CPE has numerous uniformly aligned valleys which, in turn, increase the active surface area of the modified electrode compared to the BCPE with an irregular shape, reflecting the successful modification [16]. Therefore, due to the availability of a large surface area, the BRB/CPE acts as an active electrochemical sensing platform for PA electro-oxidation.

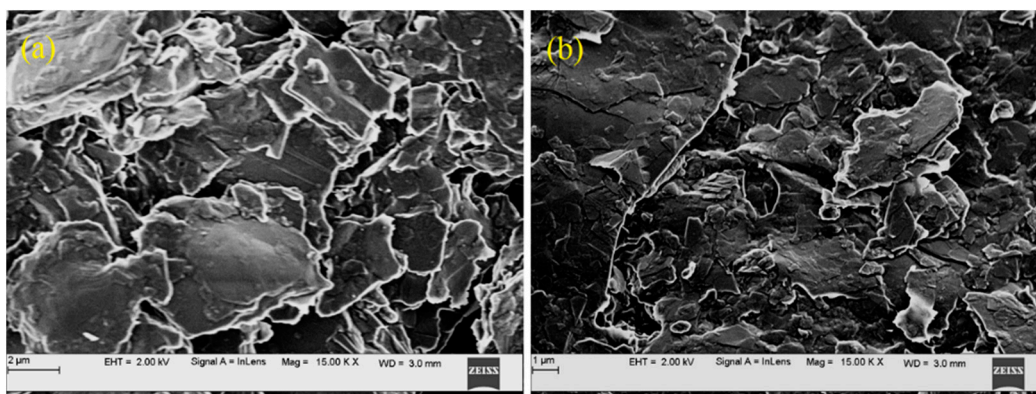


Figure 2. SEM images of BCPE (a) and BRB/CPE (b).

3.2. DFT Studies

Theoretical methods are considered as new effective and inexpensive methods to study the reactivity of molecules using density functional theory on the B3LYP with 6-31G (d,p) basis set [42]. The optimized geometries of the brilliant blue molecule as well as their frontier molecular orbitals (HOMO and LUMO) and ESP map are shown in Figure 3, while the quantum chemical descriptors extracted are summarized in Table 1.

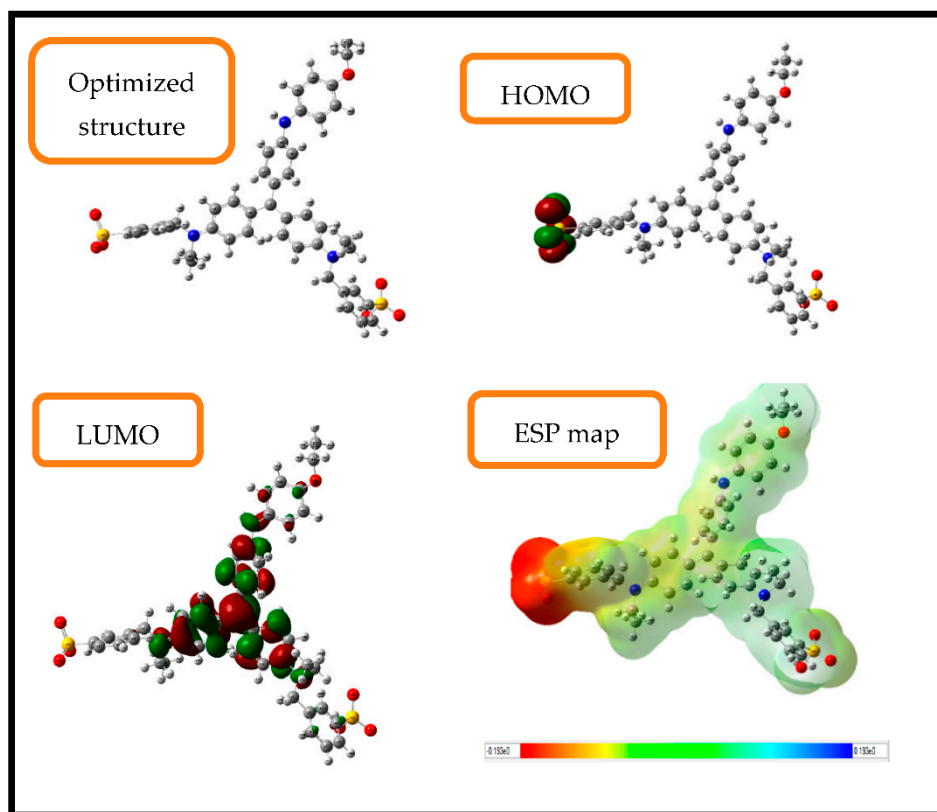


Figure 3. Optimized structure, HOMO and LUMO and ESP maps for brilliant blue molecule in aqueous phase.

Table 1. Quantum chemical descriptors for brilliant blue in aqueous phases.

Descriptors	E_{HOMO} (eV)	E_{LUMO} (eV)	ΔE_{gap} (eV)	σ (eV ⁻¹)	η (eV)	χ (eV)	ω^+	ω^-
brilliant blue	-1.9998	-0.4430	1.5567	1.2846	0.7783	1.2214	0.4448	1.6662

Firstly, it can be seen from Figure 3 that the HOMO distribution density localized on the sulfur trioxide derivative, while the LUMO density localized particularly in the center of the brilliant blue molecule. On the other hand, the electrostatic potential surface (ESP) is another way of obtaining information about the electrophilic active sites existing in the chemical species. Based on the ESP map result, it can be suggested that the electrophilic active site is localized especially in the sulfur trioxide motif since it shows a red-yellow color, indicating, therefore, the ability and the facility of the studied molecule to change and transfer electrons [43].

It is known that the high values of the HOMO orbital energies explain the ability of a molecule to donate electrons, while the low values of the LUMO orbital energy explain the ability to accept electrons. Therefore, the small value of ΔE_{gap} can be defined by a small value of energy required to remove an electron from the HOMO of the electron-donating species to the LUMO of the electron acceptor (working electrode) and make the adsorption of these molecules easier [44]. The brilliant blue molecule shows that the small energy gap might provide a higher reactivity to remove an electron from the last occupied orbital to a low unoccupied one. According to Kaya et al. [45], the chemical hardness can be defined as the resistance towards electron cloud polarization or deformation of chemical species. In other words, molecules are considered more reactive when they have a small hardness value and a high softness value, which is the case in our study. The Gazquez

parameters calculated for the studied compound showed a high electro-donating ability, with a donor capacity value of $\omega^- = 1.6662$ eV (oxidation process) and an acceptor capacity of $\omega^+ = 0.4448$ eV (reduction process) [46]. Finally, it can be concluded that the quantum global descriptors indicate that the brilliant blue structure has a high reactivity performance, which confirms their high interaction with the working electrode, explaining, therefore, the adsorption of this molecule onto the working surface electrode, forming a protective layer.

The most active sites of Fukui indices for the brilliant blue molecule were extracted in aqueous phases and are regrouped in Table 2. It can be seen from these results that the calculated values of f_k^+ are naturally localized on C1, C41, C6 and C40, which further suggests that these atoms are responsible for forming a back bond by accepting that the electron comes from the working electrode surface, while C1, C6, C5, C8 and N20 are the most active sites for the electrophilic attacks since they recorded the highest values of f_k^- . This result implies that these sites are suitable for donor–acceptor interactions and thus facilitate the adsorption of brilliant blue on the surface [47–49]. These results confirm the reactivity discussed above based on frontier molecular orbitals (HOMO, LUMO) and ESP maps.

Table 2. Most active sites of f_k^+ , f_k^- for brilliant blue in aqueous phases.

Atoms	$P(N)$	$P(N - 1)$	$P(N + 1)$	f_k^+	f_k^-
C1	6.0304	5.8997	6.1204	0.0900	0.1306
C5	6.2066	6.1458	6.2428	0.0361	0.0608
C6	5.7961	5.7063	5.8427	0.0466	0.0898
C8	6.2236	6.1612	6.2541	0.0304	0.0624
C10	5.8485	5.8101	5.8882	0.0396	0.0383
C11	6.1891	6.1567	6.2230	0.0338	0.0324
C13	6.2162	6.1914	6.2254	0.0092	0.0248
N20	7.4006	7.3407	7.4307	0.0300	0.0599
O31	9.0521	9.0142	9.0593	0.0072	0.0378
O32	9.0542	9.0145	9.0608	0.0066	0.0396
O33	9.0412	8.9955	9.0534	0.0122	0.0457
C40	6.3464	6.3447	6.3920	0.0456	0.0016
C41	6.2062	6.2046	6.2781	0.0719	0.0015
C42	6.2144	6.2068	6.2515	0.0371	0.0075
N48	7.5971	7.5771	7.5952	−0.0019	0.0200
C51	5.7175	5.6957	5.7366	0.0190	0.0218
C54	6.2649	6.2541	6.2701	0.0052	0.0107

3.3. Electrocatalytic Oxidation of PA and Effect of Scan Rate

Figure 4A represents the CVs recorded for the electro-oxidation of 20.0 μM PA in SPBS (0.2 M, pH 7.4) at BCPE (curve a) and BRB/CPE (curve b) at 0.05 Vs^{-1} . It can be observed from Figure 4A that, at BCPE, the voltammogram is relatively poor, and the oxidation potential is observed at 0.35 V (versus SCE). However, at BRB/CPE, a highly sensitive and sharp voltammetric signal is noticed at 0.34 V. Moreover, the oxidation and reduction peak potential separation for PA oxidation at the bare electrode and BRB/CPE is found to be 0.148 V and 0.036 V, respectively. This indicates the modification helps in the minimization of overpotential for PA oxidation. Therefore, these outcomes obviously reflect the superiority of the modified electrode that acts as a strong electrocatalyst for the electro-oxidation of PA at physiological pH. This significant information on the electrode phenomenon was gathered by recording the CVs at varying scan rates for the electro-oxidation of 20.0 μM PA in SPBS (0.2 M, pH 7.4) at BRB/CPE, as presented in Figure 4B. It can be noticed that as the scan rate increases, there is an enhancement in the corresponding redox current signal, with a slight shift in peak potentials. This observation is in accordance with the Randles–Sevcik relationship [16]. The linear relationships between the peak current (I_p) and scan rate (ν) and between I_p and the square root of the scan rate ($\nu^{1/2}$) are established in Figure 4C,D, respectively. The obtained correlation coefficient (r^2) for

I_{pa} versus v and I_{pc} versus v is 0.9994 and 0.9998, respectively. On the other hand, the r^2 for I_{pa} versus $v^{1/2}$ and I_{pc} versus $v^{1/2}$ is 0.9879 and 0.9834, respectively. Therefore, these results confirm the electrode phenomenon was dominated by diffusion-controlled kinetics [34,40].

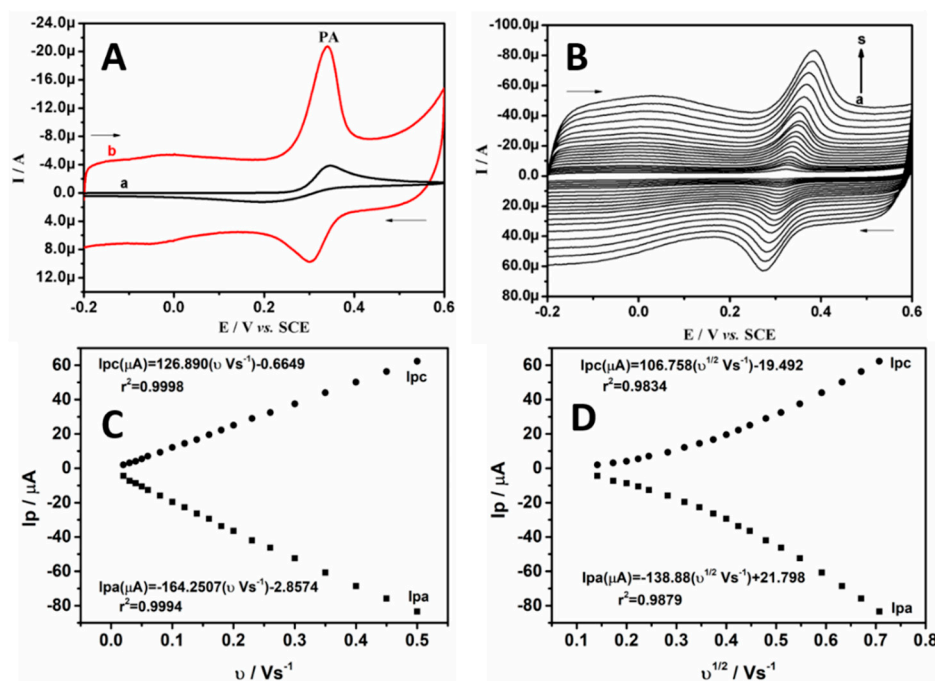


Figure 4. (A) CVs of 20.0 μM PA in SPBS (0.2 M, pH 7.4) at BCPE (curve a) and BRB/CPE (curve b) at scan rate of 0.05 Vs⁻¹. (B) CVs of 20.0 μM PA in SPBS (0.2 M, pH 7.4) at BRB/CPE with different scan rates (a-s; 0.02 Vs⁻¹ to 0.50 Vs⁻¹). (C) Linear graph of peak current of PA versus scan rate. (D) Linear graph of peak current of PA versus square root scan rate.

3.4. The Varying Concentration Effect

The influence of the varying concentration of PA at BRB/CPE was assessed by using the CV technique, as shown in Figure 5A. The enhancement in the current signal was almost proportional to an increased concentration of PA in the range of 5.0 to 30.0 μM in SPBS (0.2 M, pH 7.4) at a scan rate of 0.05 Vs⁻¹. In order to verify the linearity between the current response and concentration, a graph of I_{pa} versus the concentration of PA was established and is shown in Figure 5B, which was almost linear, and the linear regression equation was $I_{pa} (10^{-5} A) = 0.0542 (C_0 \mu M/L) + 0.9048$ ($r^2 = 0.9958$).

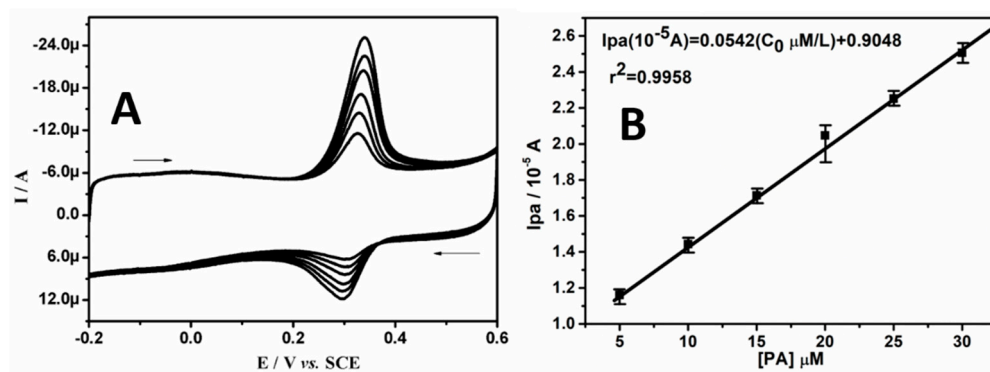


Figure 5. (A) CVs of different concentrations of PA in 0.2 M SPBS (pH 7.4) at BRB/CPE with scan rate of 0.05 Vs⁻¹. (B) Graph of anodic peak current versus concentration of PA.

Equation (10) was used to calculate the limit of detection (LOD) of PA at BRB/CPE [40,50].

$$\text{LOD} = 3 S / M \quad (10)$$

where M is the slope of the calibration graph and S is the standard deviation of the six blank measurements. The calculated LOD for PA was 0.21 μM , which is lower than most of the previous reports, as shown in Table 3 [51–63].

Table 3. Comparison of classical methods and different modified electrodes reported for electrochemical sensing of paracetamol.

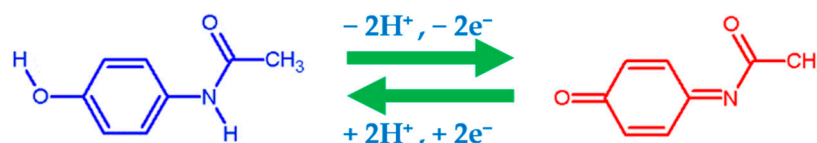
Classical Method	Working Electrode	Concentration Range (μM)	Detection Limit (μM)	References
DPV	GCE	4.0–100.0	0.369	[51]
DP-ASV	ErGO/GCE	0.2–4.4	0.25	[52]
OSWV	Cu(II)-DPM/DDT/Au	200–1500	120.0	[53]
DPV	MWCNTs/poly(Gly) GCE	0.5–10.0	0.5	[54]
DPV	SPE/PEDOT	4.0–400.0	1.39	[55]
DPV	f-MWCNTs/GCE	3.0–300.0	0.6	[56]
DPV	NC-GPE	0.2–1.3	3.71	[57]
DPV	C60/GCE	50.0–1500.0	50.0	[58]
DPV	Polypyrrole/PGE	5.0–500.0	0.79	[59]
CV	TiO ₂ /CPE	10–70.0	5.2	[60]
AdSSWV	D50wx2/GNP/GCPE	0.0334–42.2	0.0047	[61]
ATSDPV	ETPG	0.05–2.5	0.0025	[62]
DPV	35DT-GC	0.30–475.0	0.1	[63]
CV	BRB/CPE	5.0–30.0	0.21	This work

The pH of the electrolyte has a major role on the electro-oxidation of organic molecules and can be easily evaluated by recording the CV of the analyte with varying electrolyte pH. Figure S2 (see Supplementary File) shows the CVs obtained for the electro-oxidation of 20.0 μM of PA in SPBS (0.2 M) of different pH values ranging from 5.5 to 8.0. It can be noticed that the anodic peak potential (E_{pa}) of PA shifts to a negative potential due to the increased pH of SPBS. The linear establishment between E_{pa} and pH is constructed in Figure S3 (see Supplementary File), and the linear regression equation was E_{pa} (V) = 0.6324–0.0408 pH ($r^2 = 0.9926$). The obtained slope value is in agreement with the Nernstian slope of an identical number of proton and electron transfers, and the results are in agreement with a previous report [62]. On the other hand, we calculated the m/n values by using the Nernst formulae [64] given in Equation (11), where m and n are the numbers of protons and electrons, respectively. F, R and T have their scientific significance.

$$\frac{dE_p}{dpH} = \frac{2.303mRT}{nF} \quad (11)$$

The m/n value was found to be 0.712 (≈ 1) for electro-oxidation of PA, and this result confirms that the electro-oxidation of PA at BRB/CPR involves the transfer of an identical number of protons and electrons [65]. The obtained result agrees with a previous report [66]. As previously mentioned, a molecule's ability to donate electrons is explained by high HOMO orbital energies, while its ability to accept electrons is explained by low LUMO orbital energies. The Gazquez parameters calculated for the brilliant blue molecule showed a high electro-donating ability, with a donor capacity value of $\omega^- = 1.6662$ eV (oxidation process) and an acceptor capacity of $\omega^+ = 0.4448$ eV (reduction process). Therefore, the brilliant blue structure has a high reactivity performance towards the electrochemical sensing of the target analyte. Nematollahi et al. [66] proposed electro-oxidation of PA at different pH values using the CV technique. It was interpreted that the electro-oxidation might have destructed the pi bond conjugate system in PA, and

conversely for electroreduction [67]. Therefore, with the evidence of these results, the electrochemical redox pathway of PA is proposed in Scheme 1.



Scheme 1. Electro-oxidation mechanism of paracetamol.

3.5. Electrochemical Behavior of FA at BRB/CPE

Figure 6A represents the CVs of 50.0 μM of FA in SPBS (0.2 M, pH 7.4) at BCPE (curve a) and BRB/CPE (curve b) at 0.05 Vs^{-1} . It can clearly be observed that, at the bare electrode, the irreversible oxidation signal is located at 0.68 V, with poor sensitivity. However, at BRB/CPE, a highly sensitive and sharp signal is found at 0.65 V. Therefore, the modification in the bare electrode by brilliant blue improves the electrocatalytic performance towards FA determination. The increase in the oxidative peak current with the increased varying scan rate at BRB/CPE is shown in Figure 6B, for the oxidation of 30.0 μM of FA in SPBS (0.2 M, pH 7.4) in the given scan range of 0.05 to 0.225 Vs^{-1} . To assess the electrode phenomenon, graph of I_{pa} versus v and I_{pa} versus $v^{1/2}$ were plotted, which suggest the electrode phenomenon was both diffusion- and adsorption-controlled, as the correlation coefficients were 0.9989 and 0.9950, respectively, as shown in Figure 6C,D, respectively. The effect of the varying concentration of FA at the BRB/CPE was observed by recording CVs with varying concentrations of FA in the linear concentration range of 1.06×10^{-4} to 1.42×10^{-4} M, as shown in Figure 7A. The anodic peak current signal increases due to the increased concentration of FA. The linear relationship between the I_{pa} and concentration of FA with a correlation coefficient of 0.9916 suggests a linear establishment between the peak current and concentration of FA (see Figure 7B). The linear regression was $I_{\text{pa}} (10^{-5} \text{ A}) = 1.0454 (C_0 10^{-4} \text{ M/L}) + 0.70439$, ($r^2 = 0.9916$). The calculated LOD and LOQ for FA at BRB/CPE were 1.04 μM and 3.46 μM , respectively. Therefore, we can conclude that the BRB/CPE can also be used as a good electrochemical sensor for FA determination at physiological pH.

3.6. Simultaneous Electroanalysis of PA and FA

The major assignment of the BRB/CPE is, as expected, to resolve and enhance the sensitivity and selectivity in the discrimination of the targeted analytes. Figure 8 shows the CVs of 10.0 μM PA and 50.0 μM FA in SPBS (0.2 M, pH 7.4) at 0.05 Vs^{-1} . At BCPE (curve a), the oxidative signals for both PA and FA are not well defined, and the current signals are weak due to the poor performance of the BCPE. However, at BRB/CPE (curve b), two distinctive oxidation peaks with an enhanced current signal are observed at 0.318 V and 0.653 V, corresponding to PA and FA oxidation, respectively, with peak-to-peak separation of 0.335 V. Therefore, these voltammetric data show that the BRB/CPE can be used for the determination of PA in the presence of FA at physiological pH.

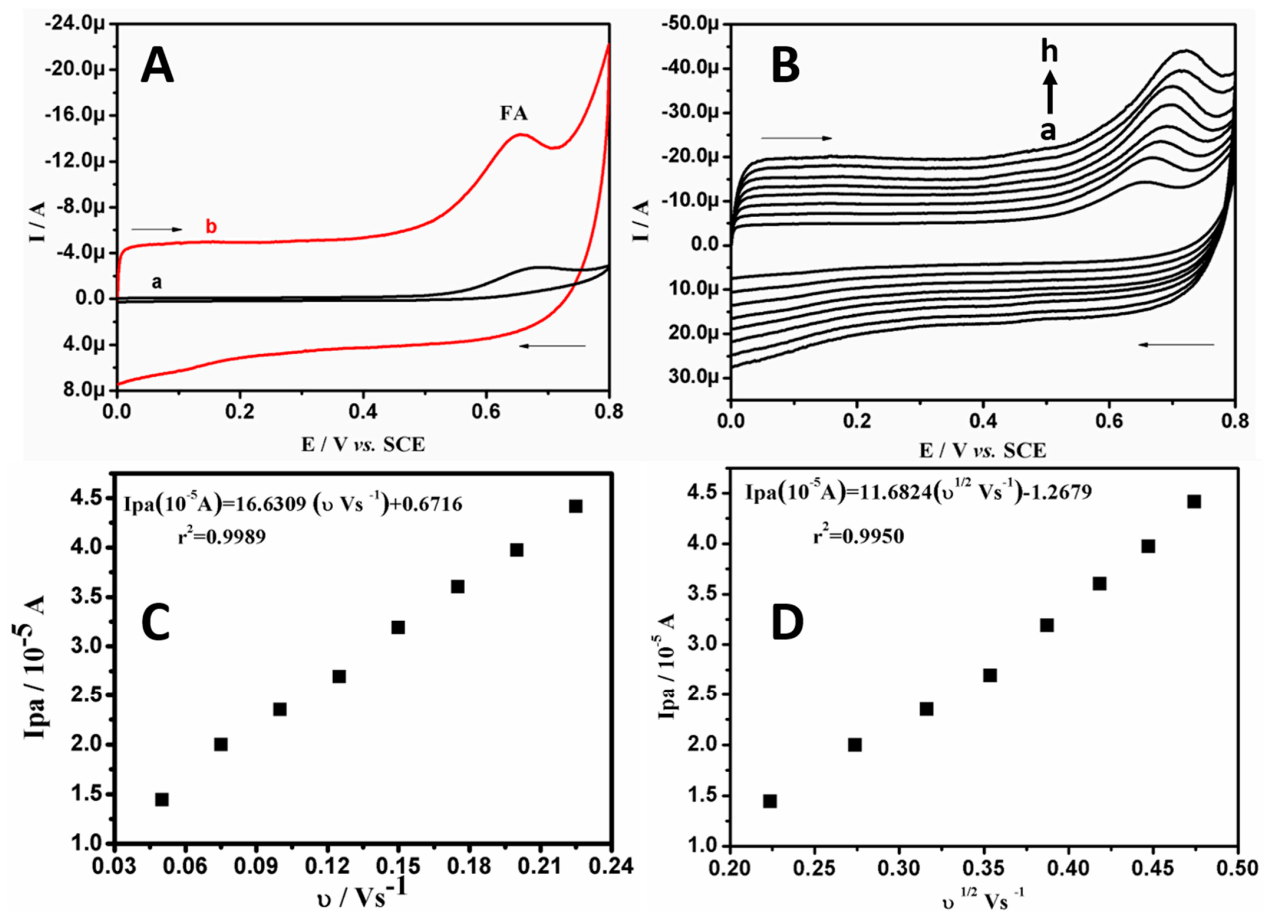


Figure 6. (A) CVs of 50.0 μM FA in SPBS (0.2 M, pH 7.4) at BCPE (curve a) and BRB/CPE (curve b) at scan rate of 0.05 Vs⁻¹. (B) CVs of 30.0 μM FA in PBS (0.2 M, pH 7.4) at BRB/CPE with different scan rates (a-h; 0.05 Vs⁻¹ to 0.225 Vs⁻¹). (C) Linear graph of peak current of FA versus scan rate. (D) Linear graph of peak current of FA versus square root scan rate.

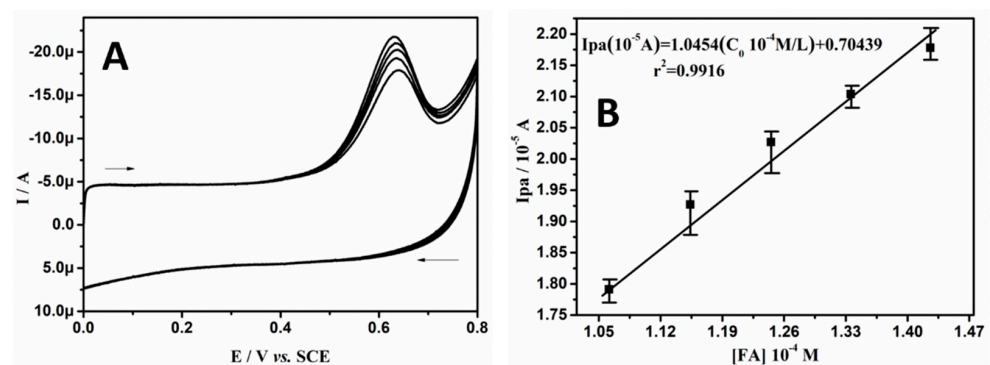


Figure 7. (A) CVs of FA in 0.2 M SPBS of pH 7.4 at BRB/CPE at scan rate of 0.05 Vs⁻¹ with different concentrations. (B) Graph of anodic peak current versus concentration of FA.

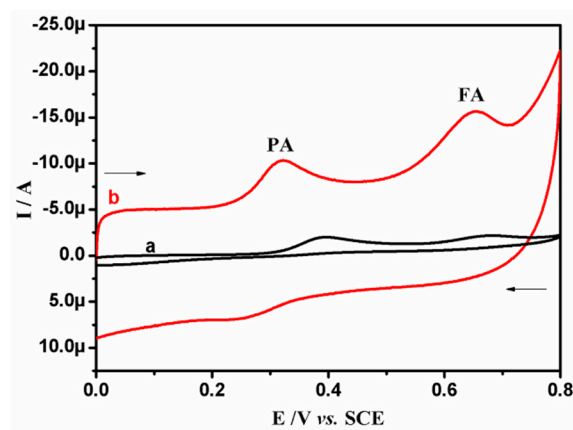


Figure 8. CVs of binary mixture containing 10.0 μM PA and 50.0 μM FA in SPBS (0.2 M, pH 7.4) at BCPE (curve a) and BRB/CPE (curve b) at scan rate of 0.05 Vs^{-1} .

3.7. Analytical Applications

The analytical application of the proposed sensor was studied by subjecting it to analysis of individual tablet samples containing PA and FA. The procedure for the tablet sample preparation is explained in Section 2.3. Table 4 shows the results of the tablet analysis at BRB/CPE. The standard recovery rates of the tablet sample were between 99.86 and 101.60% for PA and 98.80 and 100.26% for FA determination at BRB/CPE. Under the optimal conditions, the influence of interferences on the cyclic voltammogram of the binary mixture of PA and FA (20.0 μM) was investigated and is shown in Table 5. The excipients such as ascorbic acid, citric acid, oxalic acid, glucose, sucrose, lactose, glycine, sodium chloride, ammonium chloride and calcium sulphate were added tenfold in excess in the determination of PA and FA at BRB/CPE in order to judge the selectivity of the proposed protocol. The result indicates that the current signal changed slightly but did not exceed 5.0%, which justifies that the BRB/CPE is a suitable sensing platform for PA and FA and is not affected by the existence of interferences. Overall, these gathered results are acceptable and reflect the selectivity of the BRB/CPE. Therefore, the fabricated BRB/CPE can be successfully applied for the determination of analytical assays of PA and FA in pharmaceutical samples without any interferences.

Table 4. Electroanalysis of paracetamol and folic acid tablets at BRB/CPE ($n = 5$).

Tablets	Trials	Added (μM)	Found (μM)	Recovery (%)
PA	1	5.0	5.08	101.60
	2	10.0	10.03	100.30
	3	15.0	14.98	99.86
	4	20.0	20.08	100.40
FA	1	5.0	4.94	98.80
	2	10.0	9.88	98.80
	3	15.0	15.04	100.26
	4	20.0	19.89	99.45

Table 5. Influence of interferents on the voltammetric response of PA and FA.

Interferents	Concentration (mM)	Signal Change (%)	
		PA	FA
Ascorbic acid	0.2	1.24	0.91
Citric acid	0.2	1.34	0.88
Oxalic acid	0.2	1.51	0.79
Glucose	0.2	2.30	2.10
Sucrose	0.2	2.14	2.30
Lactose	0.2	1.40	2.02
Glycine	0.2	2.25	1.42
Sodium chloride	0.2	1.22	1.08
Ammonium chloride	0.2	1.26	0.98
Calcium sulphate	0.2	1.56	1.88

4. Conclusions

In order to develop an electrochemical sensor of PA and FA in pharmaceutical samples, an economical and efficient BRB/CPE sensor was fabricated. The mediating mechanism of the modifier was studied by advanced density functional theory (DFT)-based quantum chemical modeling. According to the experimental results, electrocatalytic activity was observed for PA electro-oxidation at the modified electrode involving an identical number of proton and electron transfers. The lower limit of detection was 0.21 μM by the CV method. The proposed electrode was used for the simultaneous electroanalysis of PA and FA in a binary mixture by the CV technique, and a good response was observed at the modified electrode as compared to the bare electrode. The real analytical applicability of the proposed method is valid for pharmaceutical analysis in the presence of possible excipients, suggesting that the BRB/CPE is a promising sensing platform for PA and FA detection. The methodology adopted in the present work can also be extended to the electro-oxidation of other electroactive pharmaceutical drugs.

Supplementary Materials: The following are available online at <https://www.mdpi.com/article/10.3390/chemosensors9060135/s1>, Figure S1. CVs obtained for the fabrication of BRB/CPE, 0.5 mM solution in 0.1 M NaOH (supporting electrolyte), at 15 successive cycles with scan rate of 0.1 Vs^{-1} . Figure S2. CVs obtained for the electro-oxidation of 20.0 μM PA at BRB/CPE in 0.2 M SPBS of different pH values, at scan rate of 0.05 Vs^{-1} . Figure S3. Graph of anodic peak potential versus pH of SPBS.

Author Contributions: Conceptualization, P.-S.G. and S.-Y.K.; electrode fabrication and electrochemical investigations, P.-S.G.; methodology, P.-S.G., R.S., G.S. and S.-H.L.; validation, P.-S.G., S.-Y.K., S.K. and R.S.; formal analysis, P.-S.G. and R.S.; investigation, P.-S.G., S.-Y.K., R.S. and S.K.; writing—original draft preparation, P.-S.G.; writing—review and editing, P.-S.G. and S.-Y.K.; supervision, S.-Y.K. All authors have read and agreed to the published version of the manuscript.

Funding: This work was supported by Priority Research Centers Program through the National Research Foundation of Korea (NRF) funded by the Ministry of Education (NRF-2018R1A6A1A03025526). This work was supported by the National Research Foundation of Korea (NRF) grant funded by the Ministry of Education (NRF-2020R1I1A3065371). This work was also supported by the Technology Innovation Program (10077367, Development of a film-type transparent/stretchable 3D touch sensor/haptic actuator combined module and advanced UI/UX) funded by the Ministry of Trade, Industry & Energy (MOTIE, Korea).

Institutional Review Board Statement: Not applicable.

Informed Consent Statement: Not applicable.

Data Availability Statement: Not applicable.

Conflicts of Interest: The authors declare no conflict of interest.

References

1. Jain, R.; Gupta, V.K.; Jadon, N.; Radhapyari, K. Voltammetric determination of cefixime in pharmaceuticals and biological fluids. *Anal. Biochem.* **2010**, *407*, 79–88. [[CrossRef](#)]
2. Xie, K.; Jia, Q.; Zhang, X.; Fu, L.; Zhao, G. Electronic and Magnetic Properties of Stone–Wales Defected Graphene Decorated with the Half-Metallocene of M (M = Fe, Co, Ni): A First Principle Study. *Nanomaterials* **2018**, *8*, 552. [[CrossRef](#)]
3. Gupta, V.K.; Sethi, B.; Sharma, R.; Agarwal, S.; Bharti, A. Mercury selective potentiometric sensor based on low rim functionalized thiocalix [4]-arene as a cationic receptor. *J. Mol. Liq.* **2013**, *177*, 114–118. [[CrossRef](#)]
4. Aravindan, N.; Sangaranarayanan, M.V. Differential pulse voltammetry as an alternate technique for over oxidation of polymers: Application of electrochemically synthesized over oxidized poly (Alizarin Red S) modified disposable pencil graphite electrodes for simultaneous detection of hydroquinone and catechol. *J. Electroanal. Chem.* **2017**, *789*, 148–159. [[CrossRef](#)]
5. Velmurugan, M.; Karikalan, N.; Chen, S.-M.; Cheng, Y.-H.; Karuppiah, C. Electrochemical preparation of activated graphene oxide for the simultaneous determination of hydroquinone and catechol. *J. Colloid Interface Sci.* **2017**, *500*, 54–62. [[CrossRef](#)] [[PubMed](#)]
6. Lakić, M.; Vukadinovic, A.; Kalcher, K.; Nikolić, A.S.; Stanković, D.M. Effect of cobalt doping level of ferrites in enhancing sensitivity of analytical performances of carbon paste electrode for simultaneous determination of catechol and hydroquinone. *Talanta* **2016**, *161*, 668–674. [[CrossRef](#)] [[PubMed](#)]
7. Ganesh, P.; Swamy, B.K. Simultaneous electroanalysis of norepinephrine, ascorbic acid and uric acid using poly(glutamic acid) modified carbon paste electrode. *J. Electroanal. Chem.* **2015**, *752*, 17–24. [[CrossRef](#)]
8. Tashkhourian, J.; Daneshi, M.; Nami-Ana, F.; Behbahani, M.; Bagheri, A. Simultaneous determination of hydroquinone and catechol at gold nanoparticles mesoporous silica modified carbon paste electrode. *J. Hazard. Mater.* **2016**, *318*, 117–124. [[CrossRef](#)]
9. Piovesan, J.V.; Santana, E.R.; Spinelli, A. A carbon paste electrode improved with poly(ethylene glycol) for tannic acid surveillance in beer samples. *Food Chem.* **2020**, *326*, 127055. [[CrossRef](#)]
10. Chikere, C.; Hobben, E.; Faisal, N.H.; Kong-Thoo-Lin, P.; Fernandez, C. Electroanalytical determination of gallic acid in Red and White wine samples using Cobalt Oxide Nanoparticles-modified carbon-paste electrodes. *Microchem. J.* **2020**, *160*, 105668. [[CrossRef](#)]
11. Vajdle, O.; Šekuljica, S.; Guzsavány, V.; Nagy, L.; Kónya, Z.; Ivić, M.A.; Mijin, D.; Petrović, S.; Anojčić, J. Use of carbon paste electrode and modified by gold nanoparticles for selected macrolide antibiotics determination as standard and in pharmaceutical preparations. *J. Electroanal. Chem.* **2020**, *873*, 114324. [[CrossRef](#)]
12. Xin, Y.; Wang, N.; Wang, C.; Gao, W.; Chen, M.; Liu, N.; Duan, J.; Hou, B. Electrochemical detection of hydroquinone and catechol with covalent organic framework modified carbon paste electrode. *J. Electroanal. Chem.* **2020**, *877*, 114530. [[CrossRef](#)]
13. Mahmoud, A.M.; Mahnashi, M.H.; El-Wakil, M.M. Indirect differential pulse voltammetric analysis of cyanide at porous copper based metal organic framework modified carbon paste electrode: Application to different water samples. *Talanta* **2021**, *221*, 121562. [[CrossRef](#)]
14. Santos, A.M.; Wong, A.; Almeida, A.A.; Fatibello-Filho, O. Simultaneous determination of paracetamol and ciprofloxacin in biological fluid samples using a glassy carbon electrode modified with graphene oxide and nickel oxide nanoparticles. *Talanta* **2017**, *174*, 610–618. [[CrossRef](#)]
15. Thomas, T.; Mascarenhas, R.J.; D'Souza, O.J.; Martis, P.; Dalhalla, J.; Swamy, B.K. Multi-walled carbon nanotube modified carbon paste electrode as a sensor for the amperometric detection of l-tryptophan in biological samples. *J. Colloid Interface Sci.* **2013**, *402*, 223–229. [[CrossRef](#)]
16. Ganesh, P.; Swamy, B.K. Voltammetric resolution of catechol and hydroquinone at eosin Y film modified carbon paste electrode. *J. Mol. Liq.* **2016**, *220*, 208–215. [[CrossRef](#)]
17. Šekuljica, S.; Guzsavány, V.; Anojčić, J.; Hegedűs, T.; Mikov, M.; Kalcher, K. Imidazolium-based ionic liquids as modifiers of carbon paste electrodes for trace-level voltammetric determination of dopamine in pharmaceutical preparations. *J. Mol. Liq.* **2020**, *306*, 112900. [[CrossRef](#)]
18. Zhu, M.; Li, R.; Lai, M.; Ye, H.; Long, N.; Ye, J.; Wang, J. Copper nanoparticles incorporating a cationic surfactant-graphene modified carbon paste electrode for the simultaneous determination of gatifloxacin and pefloxacin. *J. Electroanal. Chem.* **2020**, *857*, 113730. [[CrossRef](#)]
19. Mangaiyarkarasi, R.; Premlatha, S.; Khan, R.; Pratibha, R.; Umadevi, S. Electrochemical performance of a new imidazolium ionic liquid crystal and carbon paste composite electrode for the sensitive detection of paracetamol. *J. Mol. Liq.* **2020**, *319*, 114255. [[CrossRef](#)]
20. Forrest, J.A.H.; Clements, J.A.; Prescott, L.F. Clinical Pharmacokinetics of Paracetamol. *Clin. Pharmacokinet.* **1982**, *7*, 93–107. [[CrossRef](#)]
21. Olaleye, M.T.; Rocha, B.T.J. Acetaminophen-induced liver damage in mice: Effects of some medicinal plants on the oxidative defense system. *Exp. Toxicol. Pathol.* **2008**, *59*, 319–327. [[CrossRef](#)]
22. Beasley, R.; Clayton, T.; Crane, J.; von Mutius, E.; Lai, C.K.W.; Montefort, S.; Stewart, A. Association between paracetamol use in infancy and childhood, and risk of asthma, rhinoconjunctivitis, and eczema in children aged 6–7 years: Analysis from Phase Three of the ISAAC programme. *Lancet* **2008**, *372*, 1039–1048. [[CrossRef](#)]

23. Afshar, S.; Zamani, H.A.; Karimi-Maleh, H. NiO/SWCNTs coupled with an ionic liquid composite for amplified carbon paste electrode; A feasible approach for improving sensing ability of adrenalone and folic acid in dosage form. *J. Pharm. Biomed. Anal.* **2020**, *188*, 113393. [[CrossRef](#)] [[PubMed](#)]
24. Narayana, P.V.; Reddy, T.M.; Gopal, P.; Reddy, M.M.; Naidu, G.R. Electrocatalytic boost up of epinephrine and its simultaneous resolution in the presence of serotonin and folic acid at poly(serine)/multi-walled carbon nanotubes composite modified electrode: A voltammetric study. *Mater. Sci. Eng. C* **2015**, *56*, 57–65. [[CrossRef](#)] [[PubMed](#)]
25. Beitollahi, H.; Ivvari, S.G.; Torkzadeh-Mahani, M. Voltammetric determination of 6-thioguanine and folic acid using a carbon paste electrode modified with ZnO-CuO nanoplates and modifier. *Mater. Sci. Eng. C* **2016**, *69*, 128–133. [[CrossRef](#)]
26. Bayram, E.; Akyilmaz, E. Development of a new microbial biosensor based on conductive polymer/multiwalled carbon nanotube and its application to paracetamol determination. *Sens. Actuators B Chem.* **2016**, *233*, 409–418. [[CrossRef](#)]
27. Adhikari, B.-R.; Govindhan, M.; Chen, A. Sensitive Detection of Acetaminophen with Graphene-Based Electrochemical Sensor. *Electrochim. Acta* **2015**, *162*, 198–204. [[CrossRef](#)]
28. Devi, K.S.S.; Anusha, N.; Raja, S.; Kumar, A.S. A New Strategy for Direct Electrochemical Sensing of a Organophosphorus Pesticide, Triazophos, Using a Coomassie Brilliant-Blue Dye Surface-Confined Carbon-Black-Nanoparticle-Modified Electrode. *ACS Appl. Nano Mater.* **2018**, *1*, 4110–4119. [[CrossRef](#)]
29. Chen, S.; Chen, J.; Thangamuthu, R. Electrochemical Preparation of Brilliant-Blue-Modified Poly(diallyldimethylammonium Chloride) and Nafion-Coated Glassy Carbon Electrodes and Their Electrocatalytic Behavior towards Oxygen and L-Cysteine. *Electroanalysis* **2008**, *20*, 1565–1573. [[CrossRef](#)]
30. Ganesh, P.; Swamy, B.K. Simultaneous electroanalysis of hydroquinone and catechol at poly(brilliant blue) modified carbon paste electrode: A voltammetric study. *J. Electroanal. Chem.* **2015**, *756*, 193–200. [[CrossRef](#)]
31. Chandrashekar, B.N.; Lv, W.; Jayaprakash, G.K.; Harrath, K.; Liu, L.W.; Swamy, B.E.K. Cyclic Voltammetric and Quantum Chemical Studies of a Poly(methionine) Modified Carbon Paste Electrode for Simultaneous Detection of Dopamine and Uric Acid. *Chemosensors* **2019**, *7*, 24. [[CrossRef](#)]
32. Ganesh, P.-S.; Shimoga, G.; Kim, S.-Y.; Lee, S.-H.; Kaya, S.; Salim, R. Quantum chemical studies and electrochemical investigations of pyrogallol red modified carbon paste electrode fabrication for sensor application. *Microchem. J.* **2021**, *167*, 106260. [[CrossRef](#)]
33. Jayaprakash, G.K.; Swamy, B.E.K.; Chandrashekar, B.N.; Flores-Moreno, R. Theoretical and cyclic voltammetric studies on electrocatalysis of benzethonium chloride at carbon paste electrode for detection of dopamine in presence of ascorbic acid. *J. Mol. Liq.* **2017**, *240*, 395–401. [[CrossRef](#)]
34. Ganesh, P.S.; Swamy, B.E.K.; Feyami, O.E.; Ebenso, E.E. Interference free detection of dihydroxybenzene isomers at pyrogallol film coated electrode: A voltammetric method. *J. Electroanal. Chem.* **2018**, *813*, 193–199. [[CrossRef](#)]
35. Arrousse, N.; Salim, R.; Kaddouri, Y.; Zarrouk, A.; Zahri, D.; El Hajjaji, F.; Touzani, R.; Taleb, M.; Jodeh, S. The inhibition behavior of two pyrimidine-pyrazole derivatives against corrosion in hydrochloric solution: Experimental, surface analysis and in silico approach studies. *Arab. J. Chem.* **2020**, *13*, 5949–5965. [[CrossRef](#)]
36. Islam, N.; Kaya, S. (Eds.) *Conceptual Density Functional Theory and Its Application in the Chemical Domain*; CRC Press: Boca Raton, FL, USA, 2018; 422p.
37. Pearson, R.G. Absolute electronegativity and hardness: Application to inorganic chemistry. *Inorg. Chem.* **1988**, *27*, 734–740. [[CrossRef](#)]
38. Gázquez, J.L.; Cedillo, A.; Vela, A. Electrodonating and Electroaccepting Powers. *J. Phys. Chem. A* **2007**, *111*, 1966–1970. [[CrossRef](#)] [[PubMed](#)]
39. EL Hajjaji, F.; Salim, R.; Taleb, M.; Benhiba, F.; Rezki, N.; Chauhan, D.S.; Quraishi, M. Pyridinium-based ionic liquids as novel eco-friendly corrosion inhibitors for mild steel in molar hydrochloric acid: Experimental & computational approach. *Surf. Interfaces* **2021**, *22*, 100881. [[CrossRef](#)]
40. Wang, J. *Analytical Electrochemistry*; VCH Publishers: New York, NY, USA, 1994.
41. Sharp, M.; Petersson, M.; Edstrom, K. Preliminary determinations of electron transfer kinetics involving ferrocene covalently attached to a platinum surface. *J. Electroanal. Chem.* **1979**, *95*, 123–130. [[CrossRef](#)]
42. Obot, I.; Obi-Egbedi, N. Adsorption properties and inhibition of mild steel corrosion in sulphuric acid solution by ketoconazole: Experimental and theoretical investigation. *Corros. Sci.* **2010**, *52*, 198–204. [[CrossRef](#)]
43. Kaya, S.; Guo, L.; Kaya, C.; Tüzün, B.; Obot, I.; Touir, R.; Islam, N. Quantum chemical and molecular dynamic simulation studies for the prediction of inhibition efficiencies of some piperidine derivatives on the corrosion of iron. *J. Taiwan Inst. Chem. Eng.* **2016**, *65*, 522–529. [[CrossRef](#)]
44. Kaya, S.; Kaya, C. A new equation for calculation of chemical hardness of groups and molecules. *Mol. Phys.* **2015**, *113*, 1311–1319. [[CrossRef](#)]
45. Kaya, S.; Kaya, C.; Islam, N. Maximum hardness and minimum polarizability principles through lattice energies of ionic compounds. *Phys. B Condens. Matter* **2016**, *485*, 60–66. [[CrossRef](#)]
46. Jayaprakash, G.K.; Swamy, B.K.; Sánchez, J.P.M.; Li, X.; Sharma, S.; Lee, S.-L. Electrochemical and quantum chemical studies of cetylpyridinium bromide modified carbon electrode interface for sensor applications. *J. Mol. Liq.* **2020**, *315*, 113719. [[CrossRef](#)]
47. Nahlé, A.; Salim, R.; El Hajjaji, F.; Aouad, M.R.; Messali, M.; Ech-Chihbi, E.; Hammouti, B.; Taleb, M. Novel triazole derivatives as ecological corrosion inhibitors for mild steel in 1.0 M HCl: Experimental & theoretical approach. *RSC Adv.* **2021**, *11*, 4147–4162. [[CrossRef](#)]

48. Xie, K.; An, N.; Zhang, Y.; Liu, G.; Zhang, F.; Zhang, Y.; Jiao, F. Two-dimensional porphyrin sheet as an electric and optical sensor material for pH detection: A DFT study. *Comput. Mater. Sci.* **2020**, *174*, 109485. [[CrossRef](#)]
49. Zhang, Y.-H.; Li, Y.-L.; Shen, X.-R.; Xie, K.-F.; Li, T.-Y.; Zhao, J.-N.; Jia, Q.-J.; Gong, F.; Fang, S.-M. Rhombic ZnO nanosheets modified with Pd nanoparticles for enhanced ethanol sensing performances: An experimental and DFT investigation. *J. Phys. Chem. Solids* **2020**, *136*, 109144. [[CrossRef](#)]
50. Analytical Methods Committee. Recommendations for the definition, estimation and use of the detection limit. *Analyst* **1987**, *112*, 199–204. [[CrossRef](#)]
51. Engin, C.; Yilmaz, S.; Saglikoglu, G.; Yagmur, S.; Sadikoglu, M. Electroanalytical Investigation of Paracetamol on Glassy Carbon Electrode by Voltammetry. *Int. J. Electrochem. Sci.* **2015**, *10*, 1916–1925.
52. Phong, N.H.; Toan, T.T.T.; Tinh, M.X.; Tuyen, T.N.; Mau, T.X.; Khieu, D.Q. Simultaneous Voltammetric Determination of Ascorbic Acid, Paracetamol, and Caffeine Using Electrochemically Reduced Graphene-Oxide-Modified Electrode. *J. Nanomater.* **2018**, *2018*, 5348016. [[CrossRef](#)]
53. Saraswathyamma, B.; Grzybowska, I.; Orlewska, C.; Radecki, J.; Dehaen, W.; Kumar, K.G.; Radecka, H. Electroactive Dipyrromethene-Cu(II) Monolayers Deposited onto Gold Electrodes for Voltammetric Determination of Paracetamol. *Electroanalysis* **2008**, *20*, 2317–2323. [[CrossRef](#)]
54. Narayana, P.V.; Reddy, T.M.; Gopal, P.; Naidu, G.R. Electrochemical sensing of paracetamol and its simultaneous resolution in the presence of dopamine and folic acid at a multi-walled carbon nanotubes/poly(glycine) composite modified electrode. *Anal. Methods* **2014**, *6*, 9459–9468. [[CrossRef](#)]
55. Su, W.-Y.; Cheng, S.-H. Electrochemical Oxidation and Sensitive Determination of Acetaminophen in Pharmaceuticals at Poly(3,4-ethylenedioxythiophene)-Modified Screen-Printed Electrodes. *Electroanalysis* **2010**, *22*, 707–714. [[CrossRef](#)]
56. Alothman, Z.A.; Bukhari, N.; Wabaidur, S.M.; Haider, S. Simultaneous electrochemical determination of dopamine and acetaminophen using multiwall carbon nanotubes modified glassy carbon electrode. *Sens. Actuators B Chem.* **2010**, *146*, 314–320. [[CrossRef](#)]
57. Patil, M.M.; Shetti, N.P.; Malode, S.J.; Nayak, D.S.; Chakklabbi, T.R. Electroanalysis of paracetamol at nanoclay modified graphite electrode. *Mater. Today Proc.* **2019**, *18*, 986–993. [[CrossRef](#)]
58. Goyal, R.N.; Singh, S.P. Voltammetric determination of paracetamol at C60-modified glassy carbon electrode. *Electrochim. Acta* **2006**, *51*, 3008–3012. [[CrossRef](#)]
59. Özcan, L.; Şahin, Y. Determination of paracetamol based on electropolymerized-molecularly imprinted polypyrrole modified pencil graphite electrode. *Sens. Actuators B Chem.* **2007**, *127*, 362–369. [[CrossRef](#)]
60. Manjunatha, K.; Swamy, B.K.; Madhuchandra, H.; Vishnumurthy, K. Synthesis, characterization and electrochemical studies of titanium oxide nanoparticle modified carbon paste electrode for the determination of paracetamol in presence of adrenaline. *Chem. Data Collect.* **2021**, *31*, 100604. [[CrossRef](#)]
61. Sanghavi, B.J.; Srivastava, A.K. Simultaneous voltammetric determination of acetaminophen and tramadol using Dowex50wx2 and gold nanoparticles modified glassy carbon paste electrode. *Anal. Chim. Acta* **2011**, *706*, 246–254. [[CrossRef](#)] [[PubMed](#)]
62. Özcan, A.; Sahin, Y. A novel approach for the determination of paracetamol based on the reduction of N-acetyl-p-benzoquinoneimine formed on the electrochemically treated pencil graphite electrode. *Anal. Chim. Acta* **2011**, *685*, 9–14. [[CrossRef](#)]
63. Calam, T.T. Selective and Sensitive Determination of Paracetamol and Levodopa with Using Electropolymerized 3,5-Diamino-1,2,4-triazole Film on Glassy Carbon Electrode. *Electroanalysis* **2021**, *33*, 1049–1062. [[CrossRef](#)]
64. Bond, A.M. *Modern Polarographic Methods in Analytical Chemistry*; Marcle Dekkes Inc.: New York, NY, USA, 1980.
65. Laviron, E. Adsorption. Autoinhibition and Autocatalysis in Polarography and in Linear Potential Sweep Voltammetry. *J. Electroanal. Chem.* **1974**, *52*, 355–393. [[CrossRef](#)]
66. Nematollahi, D.; Shayani-Jam, H.; Alimoradi, M.; Niroomand, S. Electrochemical oxidation of acetaminophen in aqueous solutions: Kinetic evaluation of hydrolysis, hydroxylation and dimerization processes. *Electrochim. Acta* **2009**, *54*, 7407–7415. [[CrossRef](#)]
67. Hanabaratti, R.M.; Tuwar, S.M.; Nandibewoor, S.T.; Gowda, J.I. Fabrication and characterization of zinc oxide nanoparticles modified glassy carbon electrode for sensitive determination of paracetamol. *Chem. Data Collect.* **2020**, *30*, 100540. [[CrossRef](#)]